HHS Public Access

Author manuscript

Am Heart J Plus. Author manuscript; available in PMC 2023 November 17.

Published in final edited form as:

Am Heart J Plus. 2023 November ; 35: . doi:10.1016/j.ahjo.2023.100317.

Cholesterol crystals induce mechanical trauma, inflammation, and neo-vascularization in solid cancers as in atherosclerosis

George S. Abela[a,b,*], **Venkat R. Katkoori**[b], **Dorothy R. Pathak**[c], **Harvey L. Bumpers**[d], **Monika Leja**[e], **Zain ul Abideen**[a], **Manel Boumegouas**[a], **Daniel Perry**[e], **Anas Al-Janadi**[f], **James E. Richard**[g], **Carlo Barnaba**[h], **Ilce G. Medina Meza**[i]

[a]Department of Medicine, Division of Cardiology, Michigan State University, East Lansing, MI, USA

[b]Department of Physiology, Division of Pathology, Michigan State University, East Lansing, MI, USA

[c]Department of Epidemiology and Biostatistics, Michigan State University, East Lansing, MI, USA

[d]Department of Surgery, Michigan State University, East Lansing, MI, USA

[e]Department of Medicine, Division of Cardiovascular Medicine, University of Michigan, Ann Arbor, MI, USA

[f]Department of Cancer Care Services, Corewell Health, Grand Rapids, MI, USA

[g]Department of Pathology, Sparrow Hospital, Lansing, MI, USA

[h]Institute for Quantitative Health Science and Engineering, Michigan State University, East Lansing, MI, USA

[i]Biosystems and Agricultural Engineering, Michigan State University, East Lansing, MI, USA

Abstract

Background and aims: Cancer and atherosclerosis share common risk factors and inflammatory pathways that promote their proliferation via vascular endothelial growth factor (VEGF). Because CCs cause mechanical injury and inflammation in atherosclerosis, we investigated their presence in solid cancers and their activation of IL-1β, VEGF, CD44, and Ubiquityl-Histone H2B (Ub-H2B), that promote cancer growth.

[*]Corresponding author at: Michigan State University, B208 Clinical Center, East Lansing, MI 48824, USA. abela@msu.edu (G.S. Abela).

CRediT authorship contribution statement

George S. Abela: study design, methodology, investigation, project administration, supervision, data analysis, writing original draft and editing; Venkat R. Katkoori: study design, methodology, investigation, project administration, writing & editing; Dorothy R. Pathak: Study design, data analysis, writing & editing; Harvey L. Bumpers: Writing, review & editing; Monika Leja: study design, investigation; Zain ul Abideen: writing, graphics review & editing; Manel Boumegouas: investigation; Daniel Perry: investigation; Anas AI-Janadi: Writing, review & editing; James E. Richard: Investigation, data analysis; Carlo Barnaba; Investigation, data analysis; Ilce G. Medina Meza: investigation, data analysis.

Declaration of competing interest

There is no conflict of interest for any of the authors regarding this work.

Methods: Tumor specimens from eleven different types of human cancers and atherosclerotic plaques were assessed for CCs, free cholesterol content and IL1-β by microscopy, immunohistochemistry, and biochemical analysis. Breast and colon cancer cell lines were cultured with and without CCs to select for expression of VEGF, CD44, and Ub-H2B. Western blot and immunofluorescence were performed on cells to assess the effect of CCs on signaling pathways.

Results: Cancers displayed higher CC content (+2.29 ± 0.74 vs +1.46 ± 0.84, $p < 0.0001$), distribution (5.06 ± 3.13 vs 2.86 ± 2.18, $p < 0.001$) and free cholesterol (3.63 ± 4.02 vs 1.52 ± 0.56 μg/mg, $p < 0.01$) than cancer free marginal tissues and similarly for atherosclerotic plaques and margins (+2.31 ± 0.51 vs +1.44 ± 0.79, $p < 0.02$; 14.0 ± 5.74 vs 8.14 ± 5.52, $p < 0.03$; 0.19 ± 0.14 vs 0.09 ± 0.04 μg/mg, $p < 0.02$) respectively. Cancers displayed significantly increased expression of IL1-β compared to marginal tissues. CCs treated cancer cells had increased expression of VEGF, CD44, and Ub-H2B compared to control. By microscopy, CCs were found perforating cancer tumors similar to plaque rupture.

Conclusions: These findings suggest that CCs can induce trauma and activate cytokines that enhance cancer growth as in atherosclerosis.

Keywords

Cancer; Atherosclerosis; Biomarkers; Neovascularization; Cholesterol crystals

1. Introduction

The association between cancer and atherosclerosis has been previously recognized and both these common chronic conditions share many risk factors including advanced age, sedentary lifestyle, obesity, diabetes, hypercholesterolemia, smoking, and hormonal use [1–3]. Furthermore, both solid cancers and atherosclerosis derive much of their nutrients for growth via neovascularization [4,5]. These are small and fragile vessels that form mainly by the activation of vascular endothelial growth factor (VEGF) signaling. In addition, cancer and atherosclerosis share common biological responses with respect to inflammation pathways that may contribute to their progression [6–10]. This raises the possibility that cancer and atherosclerosis may also share some common enhancing agents. In previous studies on atherosclerosis, we demonstrated that cholesterol crystals (CCs) trigger an inflammatory response by activation of NOD-, LRR- and pyrin domain-containing protein 3 (NLRP3) inflammasome leading to generation of interleukin-1β (IL-1β) that cascades to activate IL-6 and then C-reactive protein by the liver [6]. A similar inflammatory process has been reported present in various cancers and with CCs in a model of colorectal cancer [7,10].

Our study investigated the presence of CCs in various solid cancers based on the hypothesis that CCs can enhance progression of cancer by inducing tissue injury and triggering inflammation as already shown in atherosclerosis [11–13]. To identify CCs induced biomarkers in cancer that involve tumor progression we proceeded to conduct in vitro cell-based studies, using breast cancer (BC) and colon cancer (CRC) cell lines exposed to CCs.

2. Methods

2.1. Patient sample collection

De-identified solid tumor cancer samples and atherosclerotic plaques with their respective marginal tissues were obtained from patients undergoing surgery.

2.2. Microscopic analysis of CCs in cancer, atherosclerosis and marginal tissues

Analysis by light microscopy (LM), scanning electron microscopy (SEM), digital 3D microscopy (DM) and confocal microscopy (CM) was performed on tissue segments from cancers, atherosclerotic plaques and corresponding marginal tissues. Since fixation does not alter CCs, tissues were fixed in 10 % neutral buffered formalin for LM, SEM and DM [14].

2.2.1. LM analysis—Fixed tissue segments were serially dehydrated with graded ethanol, embedded in paraffin blocks, cut in 5 μm sections and stained with H&E or trichrome for examination by LM. A pathologist (JER) confirmed the presence and type of the underlying cancer and the matching normal organ tissue.

2.2.2. SEM analysis—Fixed tissue samples (3 × 5 mm) were dehydrated by air drying for 24 h to preserve CCs [14,15]. Samples were mounted on stubs and gold coated in a sputter coater (EMSCOPE SC500; Emscope) and then examined using a SEM (JSM-6610LV, Jeol Ltd). CCs density was measured semi-quantitatively as absent (0), scattered few (+1), dense in a limited area (+2), or dense and widely distributed (+3) [15]. Also, the number of sites with CCs were counted and used to compare cancer and plaques versus marginal tissue in comparable size tissue segments. The average CC density per specimen was calculated by adding the individual densities from all the sites and then divided by the number of sites in a specific specimen. These crystal forms were previously confirmed to be cholesterol using energy-dispersive X-ray spectroscopy, Fourier transform infrared spectroscopy and crystal geometry [11].

2.2.3. DM analysis—Fresh fixed tissue samples were examined under the 3D Keyence VHX-6000 digital microscope (Keyence Corp, Osaka, Japan) and images of CCs obtained using a VH-Z500T high-resolution zoom lens.

2.2.4. CM analysis—Fresh unprocessed tissues were stained for CCs using cholesteryl Bodipy-C12 fluorescent dye [15]. Fluorescence images were acquired using a Zeiss Pascal LSM microscope (Carl Zeiss, Inc., Jena, Germany).

2.3. Measurement of free cholesterol quantity in cancer, atherosclerosis and marginal tissues

Cancers, atherosclerotic plaques, and their respective marginal tissues (~50–100 mg) were washed with PBS and placed in a mortar with liquid nitrogen, minced to a fine powder and then transferred to a glass tube with screwcap, 3 ml of hexane/isopropanol (4/1, v/v) and 0.1 % of BHT. Then 19-hydroxycholesterol was added as internal standard and samples sonicated for 5 min in cold water, followed by centrifugation at 2100 rpm for 5 min at 4 °C. The recovered supernatant was dried under a nitrogen stream and resuspended into 500

μl of methanol. Finally, 5 μl were injected into a 2 mm × 150 C18, 4-micron particles, 80-micron pore size (Phenomenex®) column (LC: Shimadzu Prominence (2× LC20AD pumps)). Mobile phase A: 85 % methanol + 0.1 % formic acid, mobile phase B: 100 % methanol + 0.1 % formic acid and flow rate of 250 μl/min at 50 °C. Identification of free cholesterol was obtained by comparison of fragmentation fingerprint and relative retention times of cholesterol pure standard. Quantification was performed by peak area comparison with the IS and corrected for the recovery factor. Mass spectra data were analyzed with EI-Maven package (Elucidata).

2.4. IL-1β expression in cancer tissues

RNA was isolated using the RNA Isolation Kit (NORGEN Biotek Corp). First-strand cDNA was synthesized using the First Strand cDNA Synthesis Kit (OriGene Technologies) mixed with 2× SYBR Green PCR Master Mix and gene-specific forward and reverse primers and then subjected to real-time PCR quantification. All reactions were performed in triplicate. The relative amounts of mRNAs were calculated by using the comparative cycle threshold method. All genes were normalized to the abundance of cyclophilin mRNA. Immunohistochemistry for IL1-β expression in cancer and atherosclerotic tissues was performed as previously described [16].

2.5. CCs induced biomarkers in cell culture

Cancer cell lines (MDA-MB231, MCF-7 [breast] and colon [HT29]) from American Type Culture Collection (ATCC) were cryopreserved. Cell lines were cultured in 5 % CO_2 at 37 °C in RPMI 1640 medium (Life Technologies) supplemented with L-glutamine, 10 % fetal bovine serum, and penicillin (100 U/ml)/streptomycin (100 U/ml) (Life Technologies). CCs were prepared from synthetic cholesterol (≥99 % pure, Sigma) by dissolving in ethanol and evaporating the solution (0.5 % cholesterol in 100 % ethanol) in a sterile biosafety cabinet under UV light.

2.5.1. CC treatment—Dilutions and concentrations of the CCs (2 μg/ml) were added to cell cultures that were grown to 80 % confluence and then treated with either CCs or 1 × PBS for 4 h. Immunofluorescence (IF) was performed for VEGF expression and cancer stem cell markers in lysates, by western blot (WB) a rabbit-polyclonal antibodies for VEGF (Santa Cruz Biotechnology), CD44 and Ub-H2B (Cell Signaling) were used. Methodology for IF and WB was performed as described [16]. Of note, higher concentrations of CCs were found to kill the cell lines, so the concentration used 2 μg/ml was selected as most compatible after titrations.

2.6. Statistical analysis

All analyses were performed using SAS version 9.4 (SAS Inc.). Means and standard deviations were calculated for CC density, CC sites, and free cholesterol for each of type of the cancer tissue and atherosclerotic plaque and their corresponding margin tissues where available. To test for the difference between the levels of CC density, distribution sites and free cholesterol between cancer tissue and atherosclerotic plaque and corresponding matched margin values, the Wilcoxon Signed Rank test, a nonparametric equivalent of a paired t-test, was used. To compare any un-matched cancer tissue or atherosclerotic plaque

for the three parameters under evaluation (CC density, CC sites and free cholesterol) vs. their unmatched tissue values, nonparametric Mann-Whitney test was used. A p-value ≤ 0.05 was considered statistically significant.

2.7. Ethics

The protocol “Cholesterol crystals in arterial plaque and in solid cancer tumors: A connection between coronary artery disease and cancer” #1020 was exempt by institutional review boards of Michigan State University, East Lansing, MI, University of Michigan, Ann Arbor, MI, and Sparrow Hospital, Lansing, MI.

3. Results

Extensive amounts of CCs were detected by scanning electron microscopy (SEM), confocal microscopy (CM), and digital 3D microscopy (DM) in eleven various solid cancers obtained from 76 patients including renal, colon, lung, breast, thyroid, prostate, testicular, stomach, bladder, rectal and liposarcoma. Similarly, extensive amounts of CCs were found present in all carotid artery atherosclerotic plaques obtained from 7 patients (Figs. 1–4).

3.1. Cholesterol crystal density, distribution, and free cholesterol in three cancer types with matched marginal tissues (Table 1)

For the combined results of renal, colon and lung cancers and their corresponding matched normal marginal tissues respectively, there was a significantly greater CCs density graded from +0 to +3 (+2.29 ± 0.74 vs +1.46 ± 0.84, $p < 0.0001$); number of crystal distribution sites (5.06 ± 3.13 vs 2.86 ± 2.18, $p < 0.001$); and a greater amount of free cholesterol in cancer tissue compared to normal marginal tissue (3.63 ± 4.02 vs 1.52 ± 0.56 μg/mg, $p < 0.01$).

3.2. Cholesterol crystal density, distribution, and free cholesterol in individual matched cancers and atherosclerotic plaque (Table 1)

3.2.1. Renal cell carcinoma and marginal tissue—By SEM CCs were found to be present with a significantly greater density in the renal cancer tissue compared to the matched marginal tissue (+2.29 ± 0.82 vs. +1.43 ± 0.88, $p = 0.003$). Also, the number of cholesterol crystal sites was more frequent within the renal cancer tissue compared to marginal tissue (6.00 ± 3.46 vs 3.23 ± 2.42, $p < 0.02$). Free cholesterol levels were significantly greater in the renal cancer tissue compared to the normal marginal tissue (5.83 ± 4.94 vs 1.59 ± 0.59 μg/mg, $p < 0.005$). Light microscopic analysis demonstrated that all the tumors were clear cell carcinoma, and the margins were cancer free normal renal tissue.

3.2.2. Colon cancer and marginal tissue—By SEM CCs density and number of site distribution in colon cancer were significantly greater than the normal marginal tissue but not for free cholesterol content (+2.25 ± 0.72 vs +1.38 ± 0.90, $p < 0.001$; 4.59 ± 3.06 vs 2.71 ± 2.20, $p < 0.03$; 1.71 ± 1.29 vs 1.45 ± 0.54, μg/mg; p = ns) respectively. Larger and more prominent CCs formations were found in the colon cancer compared to normal tissue. Similarly, CCs were found to be emerging from the fresh unprocessed tissue surfaces by confocal and digital microscopy (Fig. 2). Extensive fluorescence uptake of Bodipy C-12

dye by CCs was noted in carcinoma of the colon compared to normal colon (Fig. 3A). Also, by SEM extensive macrophages were occasionally found surrounding CCs and some crystals were seen dissolving with loss of sharp edge geometry (Fig. 3A, e). By LM analysis, all these tumors were adenocarcinoma (Fig. 3A, f) with some cellular differentiation and normal colon in the margins.

3.2.3. Lung cancer and marginal tissue—By SEM, in six matched cases CCs were found to be present in all samples with a higher average of CCs density and distribution in the lung cancer tissue compared to the normal marginal tissue, but this did not achieve statistical significance (+2.42 ± 0.58 vs. +1.83 ± 0.26, $p = 0.16$; 4.00 ± 1.83 vs 2.25 ± 1.26, $p = 0.25$). However, in another separate 16 matched cases (12 adenocarcinomas and 4 squamous cell carcinomas) the free cholesterol content was significantly greater in the cancer compared to the marginal tissue (0.18 ± 0.11 vs. 0.09 ± 0.07; $p < 0.0002$).

3.2.4. Atherosclerotic plaque and marginal tissue—Similar to renal and colon cancer there was a significantly greater CCs density (+2.31 ± 0.51 vs +1.44 ± 0.79, $p < 0.02$); number of crystal site distribution (14.0 ± 5.74 vs 8.14 ± 5.52, $p < 0.03$) and amount of free cholesterol in the atherosclerotic plaques compared to marginal plaque free carotid artery (0.19 ± 0.14 vs 0.09 ± 0.04 μg/mg, $p < 0.02$) (Fig. 3C).

3.3. Cholesterol crystal density, distribution in unmatched cancer samples

3.3.1. Breast cancer—By SEM, in six unmatched cases, CCs were found to be present in all samples with an average of +1.91 ± 0.23 CCs density and 7.83 ± 3.54 number of distribution sites. In one matched sample of invasive ductal carcinoma the number of crystal sites was more frequent and widely dispersed within the cancer compared to the marginal tissue (Fig. 3B). LM analysis demonstrated that these tumors were ductal carcinoma with moderate cellular differentiation.

3.3.2. Thyroid cancer—SEM analysis demonstrated extensive and widely dispersed CCs in two poorly differentiated papillary carcinoma cases (Fig. 1).

3.3.3. Prostate cancer—SEM analysis demonstrated extensive and widely dispersed CCs in two small glandular adenocarcinoma cases with some cellular differentiation (Fig. 1).

3.3.4. Other cancers—By SEM, CCs were found widely present in stomach, testicular, liposarcoma, bladder, and rectal cancer tissues.

3.4. Tissue injury

By SEM, CCs were found to be traumatizing atherosclerotic plaques with plaque rupture as well as cancers by perforating the surfaces of the tumor (Figs. 1, 2, 3A, B). Vasa vasorum in atherosclerotic plaques appeared to be surrounded by CCs with local hemorrhage (Fig. 4).

3.5. IL-1β expression in cancers

Immunohistochemistry analysis revealed that all renal, lung, prostate, thyroid, and colon cancers stained positive for IL-1β (Figs. 1, 3A, f). For colon cancer, quantitative real-time

PCR analysis indicated that cancers displayed significantly increased expression of IL-1β mRNA compared to marginal tissues (Fig. 3D).

3.6. Cholesterol crystal induced biomarkers in cancer cell lines

To evaluate the impact of CCs on activation of molecular markers that lead to neovascularization and tumor progression we tested the response of cancer cell lines to CCs using WB in BC and CRC cell lines. Cells that were exposed to CCs had a significantly increased expression of VEGF compared to unexposed cells (Fig. 3E). Immunofluorescence analysis also confirmed that CCs exposed cell lines displayed increased expression of VEGF (Fig. 3F). Moreover, CD44 and Ub-H2B that correlate with tumor recurrence, chemoresistance and tumor cell invasion had a significantly higher expression in cells exposed to CCs compared to unexposed BC and CRC cells. Normal cell function was confirmed by the presence of β-actin in both culture groups (Fig. 3E).

4. Discussion

In this study we demonstrated the presence of extensive CCs in eleven different solid cancers as is found in atherosclerotic plaques. In 1909 Charles White reported the presence of crystal shapes in fresh tumor specimens using polarizing light and subsequently others reported presence of CCs in mice tumor cultures and as clefts in basal cell carcinoma [17–19]. However, the role of CCs in cancer trauma and their extent has not been recognized or pursued and the possibility that they may influence the progression of certain cancers has not been considered.

4.1. Traumatic effects of CCs on solid cancers

Examination by digital and confocal microscopy of fresh unprocessed tissue specimens revealed presence of CCs emerging from the cancer tumor surface as seen by SEM. We have previously demonstrated that CCs perforate the fibrous caps and arterial intima that can lead to plaque rupture in patients with acute myocardial infarction [15]. In this study we found CCs perforating the surfaces of various cancer tumors suggesting that this process is similar to we had reported with plaque rupture. Moreover, this mechanical trauma can lead to local dissemination of cancer cells beyond the tumor capsule (Graphical Abstract). Also, as noted in Fig. 4, trauma to the vasa vasorum by surrounding CCs in atherosclerosis is associated with intraplaque hemorrhage [20,21]. Studies of the mechanical behavior of CCs have demonstrated that CCs can readily perforate fibrous tissues including neovascular structures [22,23]. Thus, proximity of CCs to neovascularization in tumors may cause hemorrhage within the tumor as in plaque thus facilitating cancer cell entry into the circulation and metastasis [24]. Also, in a recent report, patients who had ACS and cancer had more prominent vulnerable plaque characteristics including CCs by OCT compared to patients without cancer [25].

4.2. Free cholesterol distribution in solid cancers

Free cholesterol was found to be significantly greater in solid cancers compared to marginal tissues in kidney, squamous cell, and adenocarcinoma of the lung. Since free cholesterol is the substrate for CCs formation it supports the findings by SEM that several of the matched

cancer and marginal samples had greater amounts of CCs in the cancer. However, variability in the crystal density and distribution were noted among the different cancers which may be related to total amounts of free cholesterol content and the physicochemical conditions within the tumors.

4.3. Biochemical effects of CCs on solid cancers

In many solid tumors and atherosclerosis, VEGF is a potent angiogenic agent that promotes neovascularization leading to development and spread of cancer and atherosclerosis [4,5]. These micro-vessels surround atherosclerotic plaques, cancerous tumors and are present in diabetic retinopathy. Recently we have demonstrated that CCs activate VEGF in human retinal endothelial cells that are essential in diabetic retinopathy [26]. Moreover, VEGF targeted therapy is used as an effective chemo therapy [27].

In our study, we found extensive CCs in a variety of solid cancers and observed that CCs activate not only VEGF but also CD44 and Ub-H2B in three cancer cell lines compared to control without CCs. Numerous cellular activities involving proliferation and metastasis are enhanced by CD44 and Ub-H2B [28,29]. However, until the current study the role CCs activating VEGF, CD44 and Ub-H2B in cancer cell lines has not been previously demonstrated.

4.4. Common inflammatory mechanism in atherosclerosis and cancers

Since both atherosclerosis and cancer share similar risk factors, they seem to also share similar injurious agents. Moreover, other crystals including uric acid crystals, silicates, and airborne inhaled particulates have all been shown to trigger a similar inflammatory pathway via NLRP3 [6,30,31] and some (asbestos, silica) can be carcinogenic [32]. Thus, crystalloids that overwhelm the immune system by either mass effect or that cannot be degraded by scavenger cells can pose a constant irritation leading to an iterative cycle of inflammatory injury that may in certain instances promote carcinogenesis, and in the arterial wall contribute to persistent cardiovascular risk [33]. In this study, some of the colon cancers had extensive macrophage aggregates surrounding CCs and dissolving them indicating that they were being sensed as foreign. This is similar to what we observed in aspirates from some of the culprit coronary arteries during myocardial infarction where macrophages were found to be engaging and degrading CCs [11].

Our prior research demonstrated that CCs triggers the innate immune system via NLRP3 inflammasome leading to the activation of IL-1β in atherosclerosis [6]. One prior study reported that IL-1β is present in cancerous tumors associated with CCs [10] while others have reported that it may have an important role in tumorigenesis and metastasis [9,34]. This suggests that some cancers and atherosclerosis share this common inflammatory pathway and our study points to CCs as an agent that may contribute to the expression of IL-1β that triggers inflammation in these cancers as has been shown in atherosclerosis [6,11].

4.5. Future prospects for common treatment targets for atherosclerosis and cancers

Aspirin and statins are well established in the treatment of atherosclerotic disease, but many studies have also reported their ability to reduce the incidence of cancer, especially

when used for many years. Also, recently, colchicine was approved for prevention treatment of patients with existing and those with multiple risk factors for cardiovascular disease based on the Lodoco study [35,36]. Moreover, we have found that both aspirin, statins and colchicine can inhibit the growth and expansion of CCs in vitro as well as in vivo for statins [37–39]. This suggests that some of the benefits derived from aspirin, colchicine and statins in atherosclerosis and cancer may be related in part to their inhibition of crystal formation, dissolution of CCs and reduced associated inflammation.

4.6. Limitations

A limitation of this study is the small number of marginal tissues available with some cancers, like breast, to conduct matched comparisons. However, when combining tumors, CCs are more frequently distributed in the cancer versus the marginal tissue and free cholesterol was more abundant in the cancers as well. For lung tumors, not enough tissue was available to evaluate both the CCs by SEM and free cholesterol measurements on the same segments. Also, clinical data was not available that could have added further insight into the various tumor specimen lipid composition and hence CCs content.

5. Conclusion

In this report, we draw attention to the injurious and inflammatory effects of CCs that can contribute to the progression of both cancer and atherosclerosis. CCs induced tumor trauma can lead to dissemination of cancer cells both locally and by metastasis via neovascular injury. This process is similar to how CCs puncture fibrous caps leading to plaque rupture. We demonstrate extensive accumulation of CCs in 11 solid tumors. This is the first report to provide quantification and distribution of CCs in cancer tumors with activation of VEGF, CD44 and Ub-H2B that can contribute to the progression of malignancies and enhance their growth.

These findings highlight a fundamental relationship between cancer and atherosclerosis. Further research in vivo studies to identify shared connections and common treatment targets between these two conditions will help develop strategies to treat cancer patients or those at high risk as a prevention. These data may introduce additional therapies for the treatment of solid cancers that inhibit CCs formation which appears to enhance tumor growth. The relationship between atherosclerosis and cancer is elucidated by these findings that underscore the role of CCs in both conditions.

Acknowledgements

The authors thank Abigail Vanderberg Center for Advanced Microscopy for scanning and digital microscopy and Amy Porter, Investigative Histopathology Laboratory for light microscopy. They thank Dr. Ara Pridjian, Thoracic Surgery, Sparrow Hospital for providing the atherosclerotic carotid plaques. Also, they thank Mark Schnepp at the Sparrow Hospital Pathology Lab, Lansing, MI and the pathology lab at the University of Michigan, Ann Arbor, MI for collecting cancer specimens.

Funding

Funding was provided by Michigan State University Department of Medicine seed fund; The Jean P. Schultz Biomedical Research Endowment, Michigan State University and Edward W. Sparrow Hospital, Lansing, MI; National Institutes of Health grant 2 R01 EY025383-05A1.

Abbreviations

CCs	Cholesterol crystals
BC	Breast cancer cells
CRC	Colon cancer cells
CM	Confocal microscopy
DM	Digital 3D microscopy
IL-1β	Interleukin-1β
IF	Immunofluorescence
LM	Light microscopy
SEM	Scanning electron microscopy
Ub-H2B	Ubiquityl-Histone H2B
VEGF	Vascular endothelial growth factor
WB	Western blot

References

[1]. Tapia-Vieyra JV, Delgado-Coello B, Mas-Oliva J, Atherosclerosis and cancer; a resemblance with far-reaching implications, Arch. Med. Res 48 (2017) 12–26. [PubMed: 28577865]

[2]. Calle EE, Rodriguez C, Walker-Thurmond K, Thun MJ, Overweight, obesity, and mortality from cancer in a prospectively studied cohort of U.S. adults, N. Engl. J. Med 348 (2003) 1625–1638. [PubMed: 12711737]

[3]. Koene RJ, Prizment AE, Blaes A, et al. , Shared risk factors in cardiovascular disease and cancer, Circulation 133 (2016) 1104–1114. [PubMed: 26976915]

[4]. Xu J, Lu X, Shi GP, Vasa vasorum in atherosclerosis and clinical significance, Int. J. Mol. Sci 16 (2015) 11574–11608. [PubMed: 26006236]

[5]. Katayama Y, Uchino J, Chihara Y, et al. , Tumor neovascularization and developments in therapeutics, Cancers (Basel) 11 (2019) 316. [PubMed: 30845711]

[6]. Düewell P, Kono H, Rayner KJ, et al. , NLRP3 inflammasomes are required for atherogenesis and activated by cholesterol crystals, Nature 464 (2010) 1357–1361. [PubMed: 20428172]

[7]. Lewis AM, Varghese S, Xu H, et al. , Interleukin-1 and cancer progression: the emerging role of interleukin-1 receptor antagonist as a novel therapeutic agent in cancer treatment, J. Transl. Med 4 (2006) 48. [PubMed: 17096856]

[8]. Grivennikov SI, Greten FR, Karin M, Immunity, inflammation, and cancer, Cell 140 (2010) 883–899. [PubMed: 20303878]

[9]. Apte RN, Dotan S, Elkabets M, et al. , The involvement of IL-1 in tumorigenesis, tumor invasiveness, metastasis and tumor-host interactions, Cancer Metastasis Rev. 25 (2006) 387–408. [PubMed: 17043764]

[10]. Du Q, Wang Q, Fan H, et al. , Dietary cholesterol promotes AOM-induced colorectal cancer through activating the NLRP3 inflammasome, Biochem. Pharmacol 105 (2016) 42–54. [PubMed: 26921636]

[11]. Abela GS, Kalavakunta JK, Janoudi A, et al. , Frequency of cholesterol crystals in culprit coronary artery aspirate during acute myocardial infarction and their relation to inflammation and myocardial injury, Am. J. Cardiol 120 (2017) 1699–1707. [PubMed: 28867129]

[12]. Patel R, Janoudi A, Vedre A, et al. , Plaque rupture and thrombosis are reduced by lowering cholesterol levels and crystallization with ezetimibe and are correlated with fluorodeoxyglucose positron emission tomography, Arterioscler. Thromb. Vasc. Biol 31 (2011) 2007–2014. [PubMed: 21817102]

[13]. Libby P, Inflammation in atherosclerosis, Nature 420 (2002) 868–874. [PubMed: 12490960]

[14]. Nasiri M, Janoudi A, Vanderberg A et al. , Role of cholesterol crystals in atherosclerosis is unmasked by altering tissue preparation methods, Microsc. Res. Tech 78 (2015) 969–974. [PubMed: 26278962]

[15]. Abela GS, Aziz K, Vedre A, et al. , Effect of cholesterol crystals on plaques and intima in arteries of patients with acute coronary and cerebrovascular syndromes, Am. J. Cardiol 103 (2009) 959–968. [PubMed: 19327423]

[16]. Katkoori VR, Basson MD, Bond VC, et al. , Nef-M1, a peptide antagonist of CXCR4, inhibits tumor angiogenesis and epithelial to mesenchymal transition in colon and breast cancers, Oncotarget 6 (2015) 27763–27777. [PubMed: 26318034]

[17]. White CP, On the occurrence of crystals in tumours, J. Pathol. Bacteriol 13 (1909) 1–10.

[18]. Richters A, Sherwin RP, The occurrence of biologic crystals in tumor and nontumor cultures of C3H/HeJ mice, Cancer Res. 25 (1965) 214–219. [PubMed: 14268438]

[19]. Okamura K, Konno T, Kawaguchi M, et al. , Cholesterol crystal deposition in basal cell carcinoma: an investigation of 4 cases, J. Cosmet. Dermatol. Sci. Appl 5 (2015) 176–180.

[20]. Abela GS, Cholesterol crystals piercing the arterial plaque and intima trigger local and systemic inflammation, J. Clin. Lipidol 4 (2010) 156–164. [PubMed: 21122648]

[21]. Mughal MM, Khan MK, DeMarco JK, et al. , Symptomatic and asymptomatic carotid artery plaque, Expert. Rev. Cardiovasc. Ther 9 (2011) 1315–1330. [PubMed: 21985544]

[22]. Abela GS, Aziz K, Cholesterol crystals rupture biological membranes and human plaques during acute cardiovascular events - a novel insight into plaque rupture by scanning electron microscopy, Scanning 28 (2006) 1–10. [PubMed: 16502619]

[23]. Al-Handawi MB, Commins P, Karothu DP, et al. , Mechanical and crystallographic analysis of cholesterol crystals puncturing biological membranes, Chem. Eur. J 24 (2018) 11493–11497. [PubMed: 29877594]

[24]. Valastyan S, Weinberg RA, Tumor metastasis: molecular insights and evolving paradigms, Cell 147 (2011) 275–292. [PubMed: 22000009]

[25]. Wang C, Tian X, Feng X, et al. , Pancoronary plaque characteristics and clinical outcomes in acute coronary syndrome patients with cancer history, Atherosclerosis (2023), 10.1016/j.atherosclerosis.2023.03.023 (S0021-9150(23)00140-5).

[26]. Hammer SS, Dorweiler TF, McFarland D, et al. , Cholesterol crystal formation is a unifying pathogenic mechanism in the development of diabetic retinopathy, Diabetologia. 66 (9) (2023) 1705–1718, 10.1007/s00125-023-05949-w. [PubMed: 37311879]

[27]. Ferrara N, Hillan KJ, Novotny W, Bevacizumab (Avastin), a humanized anti-VEGF monoclonal antibody for cancer therapy, Biochem. Biophys. Res. Commun 333 (2005) 328–335. [PubMed: 15961063]

[28]. Gao Y, Foster R, Yang X, et al. , Up-regulation of CD44 in the development of metastasis, recurrence and drug resistance of ovarian cancer, Oncotarget 6 (11) (2015) 9313–9326. [PubMed: 25823654]

[29]. Espinosa JM, Histone H2B ubiquitination: the cancer connection, Genes Dev. 22 (2008) 2743–2749. [PubMed: 18923072]

[30]. Hornung V, Bauernfeind F, Halle A, et al. , Silica crystals and aluminum salts activate the NALP3 inflammasome through phagosomal destabilization, Nat. Immunol 9 (2008) 847–856. [PubMed: 18604214]

[31]. Rajagopalan S, Al-Kindi SG, Brook RD, Air pollution and cardiovascular disease: JACC state-of-the-art review, J. Am. Coll. Cardiol 72 (2018) 2054–2070. [PubMed: 30336830]

[32]. LaDou J, The asbestos cancer epidemic, Environ. Health Perspect 112 (2004) 285–290. [PubMed: 14998741]

[33]. Nidorf SM, Fiolet A, Abela GS, Viewing atherosclerosis through a crystal lens: how the evolving structure of cholesterol crystals in atherosclerotic plaque alters its stability, J. Clin. Lipidol 14 (2020) 619–630. [PubMed: 32792218]

[34]. Tulotta C, Ottewell P, The role of IL-1β in breast cancer bone metastasis, Endocr. Relat. Cancer 25 (2018) R421–R434. [PubMed: 29760166]

[35]. Nidorf SM, Fiolet ATL, Mosterd A, et al. , Colchicine in patients with chronic coronary disease, N. Engl. J. Med 383 (2020) 1838–1847. [PubMed: 32865380]

[36]. FDA Reference ID: 5192662. Accessdata.fda.gov.

[37]. Fry L, Lee A, Khan S, et al. , Effect of aspirin on cholesterol crystallization: a potential mechanism for plaque stabilization, Am. Heart J. Plus Cardiol. Res. Pract 13 (2022), 100083.

[38]. Abela GS, Hammer S, Huang X, et al., Agents that affect cholesterol crystallization and modify the risk of crystal induced traumatic and inflammatory injury, in: Abela GS, Nidorf SM (Eds.), Cholesterol Crystals in Atherosclerosis and Other Related Diseases, NY. Springer/Nature, New York, 2023 (in press).

[39]. Abela GS, Vedre A, Janoudi A, et al. , Effect of statins on cholesterol crystallization and atherosclerotic plaque stabilization, Am. J. Cardiol 107 (2011) 1710–1717. [PubMed: 21507364]

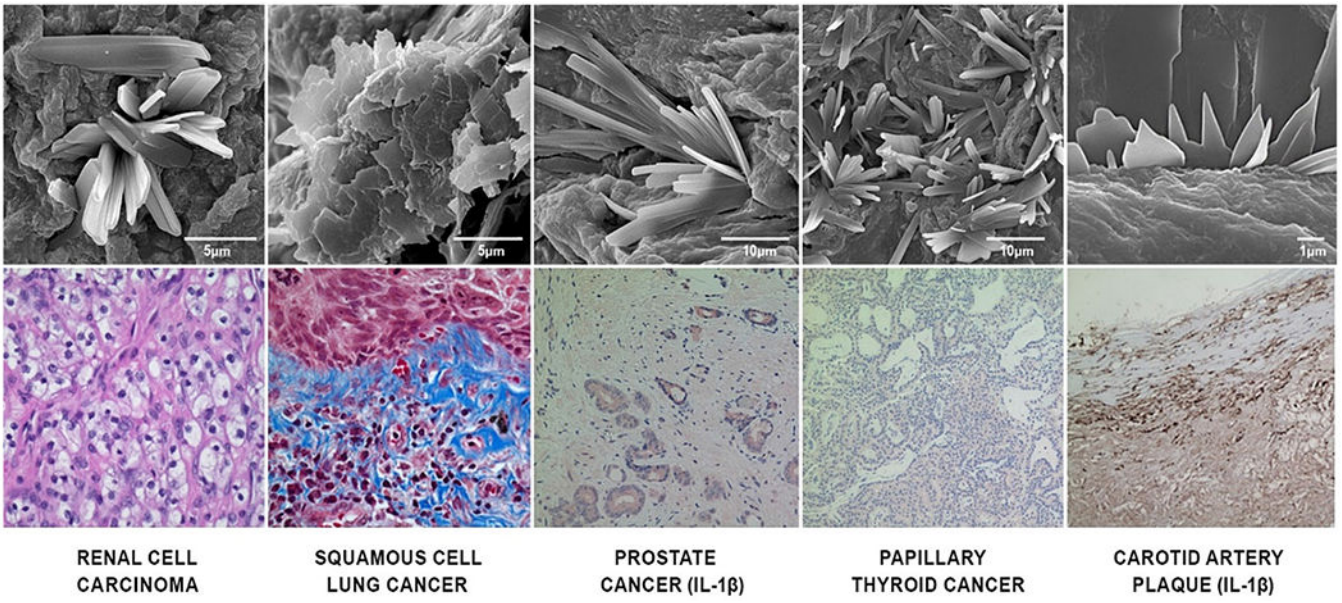

Fig. 1.

Scanning and light microscopy of cancer and atherosclerosis: (Top row) Scanning electron micrographs of various cancers and carotid plaque demonstrating presence of extensive cholesterol crystals perforating the tumor and plaque surface. (Bottom row) Matched cancer type is confirmed by light microscopy. Also, immunostaining for IL-1β demonstrating its presence in prostate cancer and atherosclerotic plaque.

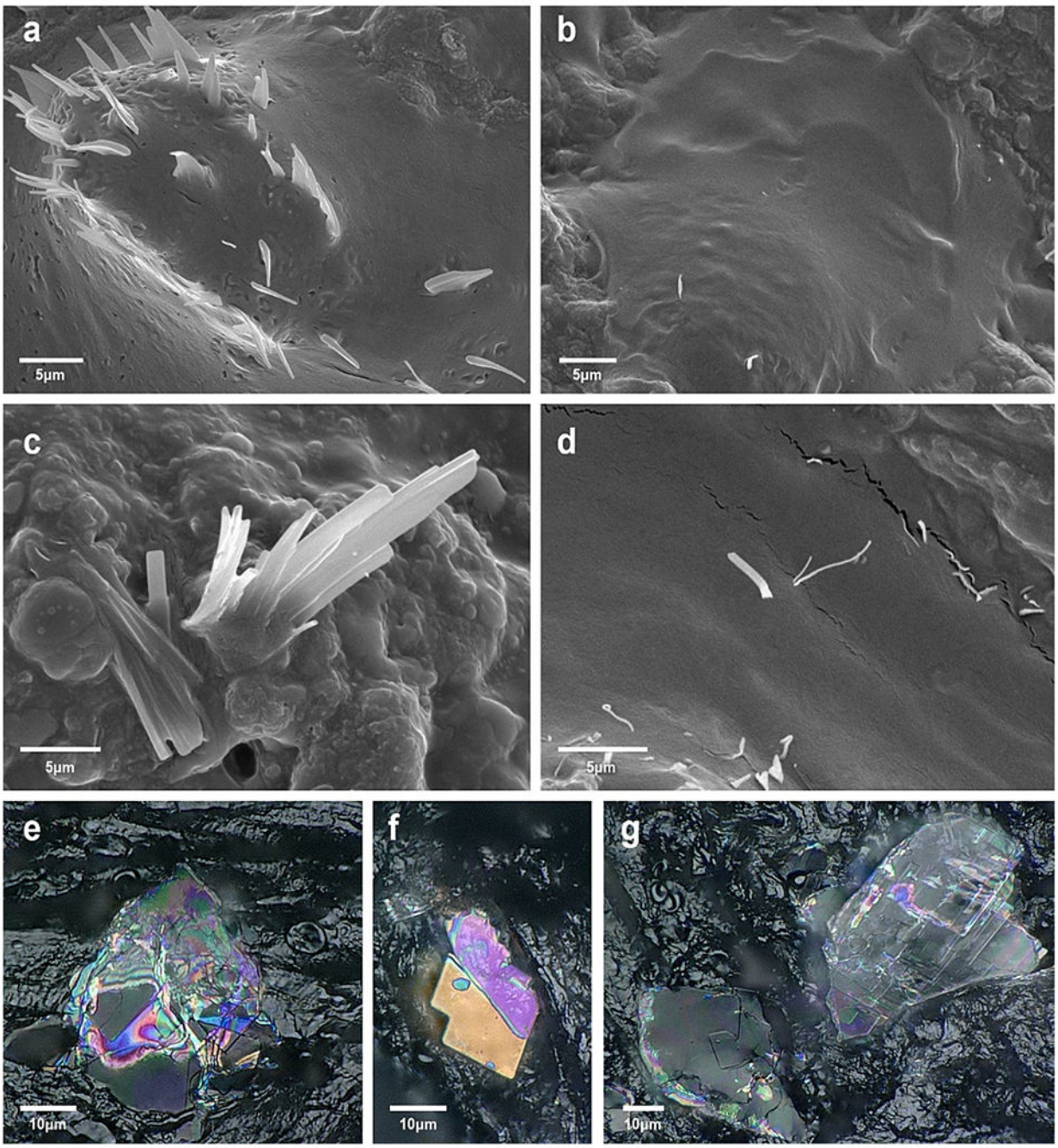

Fig. 2.

Scanning and 3D-digital microscopy of colon cancer and marginal tissue: Scanning electron micrographs of colon cancer (a, c) and matching marginal tissue (b, d) demonstrate larger and prominent cholesterol crystal formations in the cancer but not in the normal marginal tissue. CCs are seen traumatizing and perforating the tumor surface. Digital microscopy of fresh unprocessed tissue demonstrates the presence of large cholesterol crystal formations in the colon cancer (e, f, g).

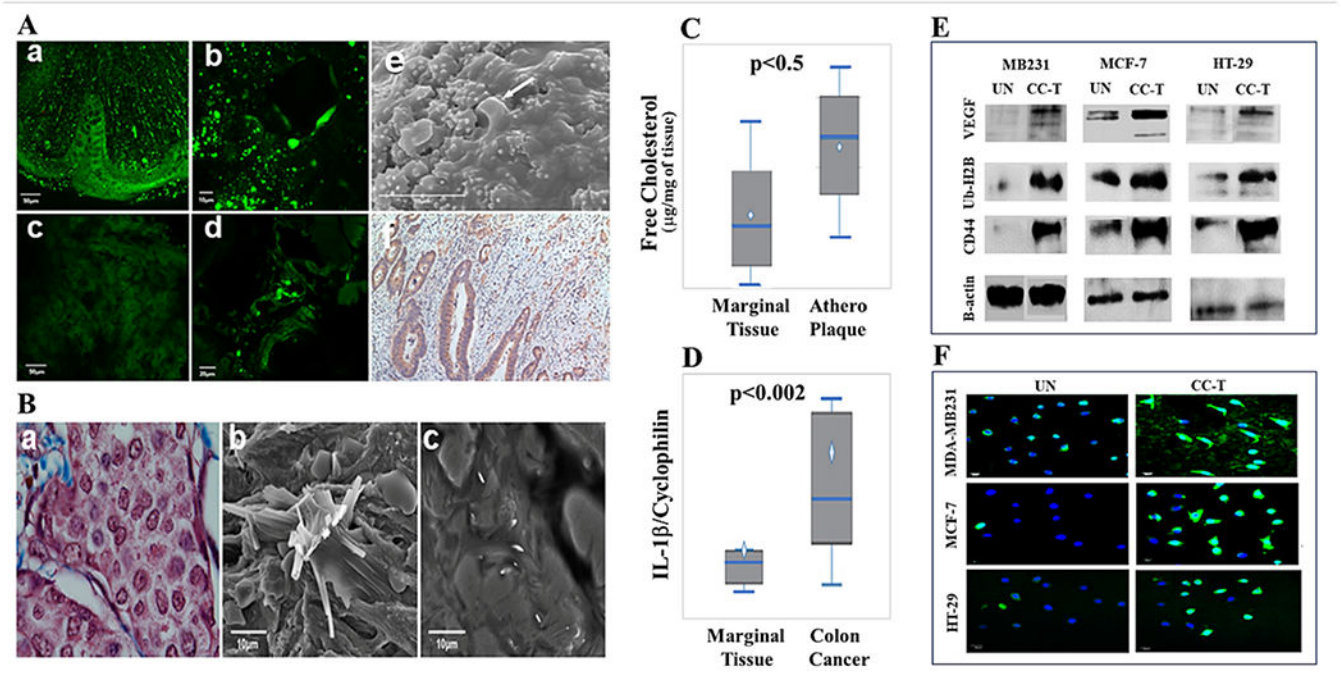

Fig. 3.

Scanning, light, confocal microscopy and cytokine activation: Extensive fluorescence uptake of Bodipy C-12 dye by CCs is noted in carcinoma of the colon (A, a, b, d) but not in the matched marginal colon without CCs (A, c). SEM demonstrates extensive macrophages surrounding a cholesterol crystal that appears dissolving (arrow, A, e). LM demonstrates positive IL-1β stain of adenocarcinoma of the colon (A, f). Ductal cell carcinoma of the breast is confirmed by LM (B, a). SEM of matched breast cancer and marginal tissue demonstrates extensive CCs in the tumor perforating the surface (B, b) but not in the surrounding marginal tissue (B, c). IL-1β mRNA expression in colon cancer tissues is significantly (average fold change: 109 [marginal tissue] vs. 304 [colon cancer]) greater compared to normal marginal tissues (C). Free cholesterol content in carotid plaques is significantly greater compared to the surrounding tissue margins and normal arteries (D). In vitro cell based studies by western blot and green immunofluorescence demonstrate CCs (UT vs. CC-T) induces increased expression of VEGF (immunofluorescence and western blot) and cancer stem cell markers (western blot) in both breast and colon cancer cell lines (E, F). Athero = atherosclerotic CCs = cholesterol crystals; LM = light microscopy; SEM = Scanning electron microscopy; UT = untreated; CC-T = Cholesterol crystal treated.

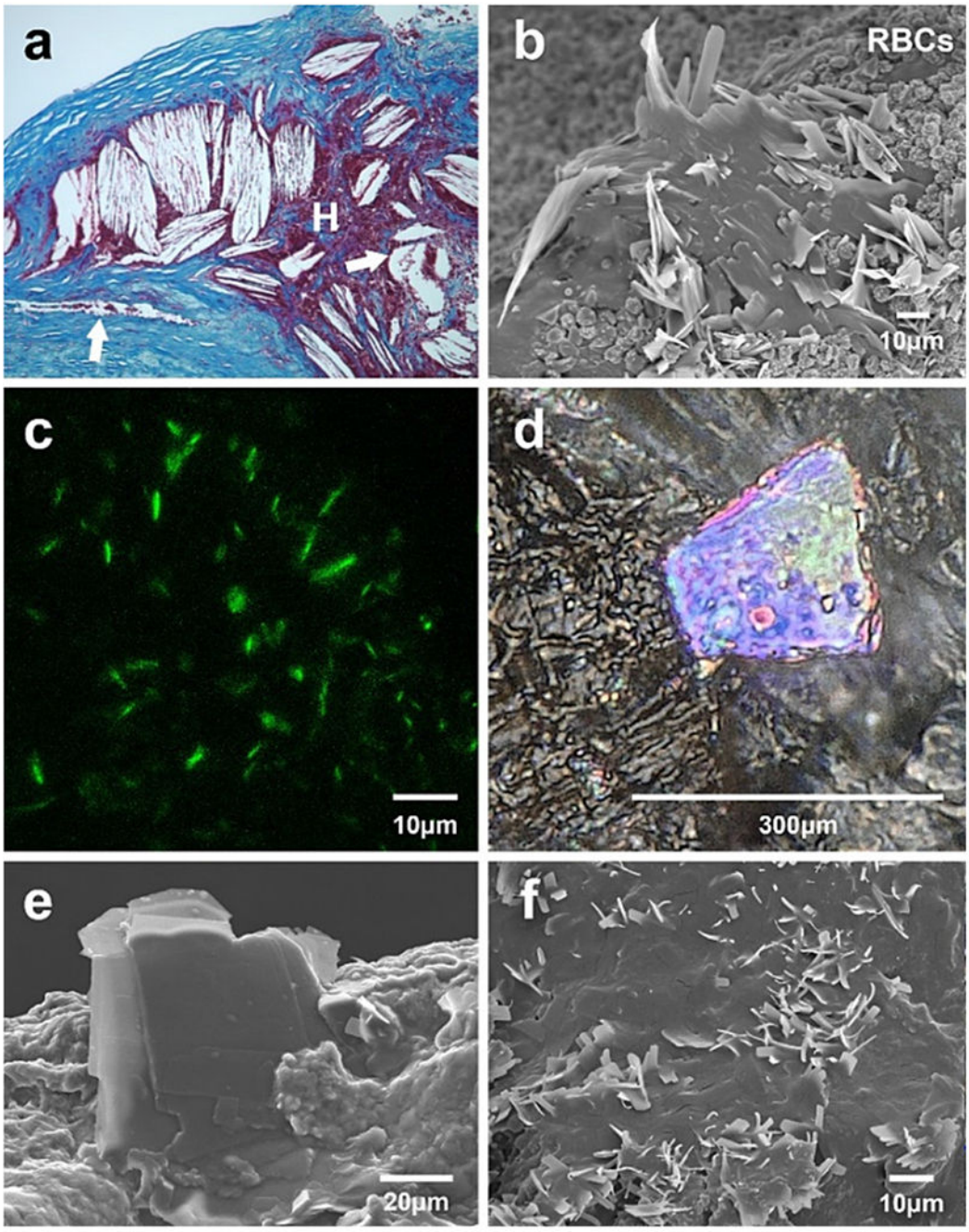

Fig. 4.

Mechanical trauma with hemorrhage by cholesterol crystals in atherosclerosis: a) Light micrograph of CCs in atherosclerotic plaque with rupture and hemorrhage; vasa vasorum (arrows) is surrounded by CCs and extravasated blood (H); b) by scanning electron microscopy crystals are noted emerging from the plaque surface surrounded by RBCs; c) fluorescence microscopy reveals CCs studded over the plaque surface; d) by digital microscopy CCs are seen emerging at the plaque surface; e) SEM at higher magnification of

a large rhomboid CC emerging form the plaque surface during acute cardiovascular even; f) SEM at lower magnification many CCs are seen perforating the surface of a carotid plaque.

Table 1

Cholesterol crystal density, distribution, and free cholesterol levels in cancer and atherosclerosis in matched tissues.

Tissue type	Crystal density (mean ± sd)				Crystal distribution (mean ± sd)				Free cholesterol (μg/mg) (mean ± sd)			
	n	Lesion	Margin	p-Value	n	Lesion	Margin	p-Value	n	Lesion	Margin	p-Value
Renal cancer	(21)	+2.29 ±0.82	+1.43 ±0.88	0.003	(13)	6.00 ±3.46	3.23 ±2.42	0.02	(14)	5.83 ±4.94	1.59 ±0.59	0.005
Colon cancer	(20)	+2.25 ±0.72	+1.38 ±0.90	0.001	(17)	4.59 ±3.06	2.71 ±2.20	0.03	(15)	1.74 ±1.33	1.45 ±0.54	0.978
Lung cancer	(6)	+2.42 ±0.58	+1.83 ±0.26	0.16	(4)	4.00 ±1.83	2.25 ±1.26	0.25	–	–	–	–
	–	–	–	–	–	–	–	–	(16)	0.18 ±0.11	0.09 ±0.07	0.0002
Combined renal, lung, and colon cancers	(47)	+2.29 ±0.74	+1.46 ±0.84	0.0001	(34)	5.06 ±3.13	2.86 ±2.18	0.001	(45)	2.46 ±3.67	1.01 ±0.82	0.005
Atherosclerotic plaque	(7)	+2.31 ±0.51	+1.44 ±0.79	0.02	(7)	14.0 ±5.74	8.14 ±5.74	0.03	–	–	–	–
	–	–	–	–	–	–	–	–	(17)	0.19 ±0.14	0.09 ±0.04	0.02

n = number of cases, sd = standard deviation, – no available data.